CHALLENGES IN EUROPEAN AEROSPACE
5TH CEAS AIR & SPACE CONFERENCE

Characteristics of locked and free-wheeling ducted fan based on wind tunnel tests and CFD analyses

Krzysztof Bogdański
Warsaw University of Technology, Poland
M.Sc., Ph.D student,
Plac Politechniki 1, 00-661, Warsaw, mazowieckie, Poland
kbogdanski@meil.pw.edu.pl

Mirosław Rodzewicz
Warsaw University of Technology, Poland

Paweł Ruchała
Institute of Aviation, Warsaw, Poland

ABSTRACT

The article describes locked and free-wheeling characteristics of a ducted fan propulsion system based on wind tunnel and computational fluid dynamics (CFD) analyses. The ducted fan unit is a propulsion system in a pusher configuration especially designed for a dynamically scale model of a new generation aircraft built in a joined wing configuration. Due to the recent development in electric propulsion systems, new possibilities are arising. Stopping and restarting the motor in flight allows better determination of aircraft performance (for example lift to drag ratio) during flight tests of dynamically scale flight models. Tests of free-wheeling and locked ducted fan and unshrouded propellers for comparison have been performed in different conditions.

INTRODUCTION

Presented research has been carried out under program concerning design, build and tests of an unmanned airplane in a joined wing configuration MOSUPS (Fig. 1). One of the parts of the research concerns the design and integration of the propulsion system with the aircraft. In order to fully determine the characteristics of the ducted fan designed for the airplane, wind tunnel tests have been conducted.

This research focuses on the freewheeling and locked characteristics of the propulsion system, which is especially useful in the determination of aircraft performance (while landing or with low speed flight) and when creating safety procedures for emergency situations (when the engine/motor quits).

Fig. 1. MOSUPS aircraft on its maiden flight with unshrouded propeller

1. DUCTED FAN UNITS

Presented propulsion system has been specially designed for MOSUPS unmanned aerial vehicle. MOSUPS is a new generation of joined wing configuration with a wingspan of 3m and maximum take-off weight of less than 25kg. Due to the use of pusher configuration the diameter of the propeller should be minimalized and the propeller itself should be protected during take-off and landing. This naturally leads to ducted fan as the optimal option. Additional advantages of ducted fans include better efficiency than typical unshrouded propellers for speeds up to 45m/s. First version of the ducted fan has been presented in Fig.2

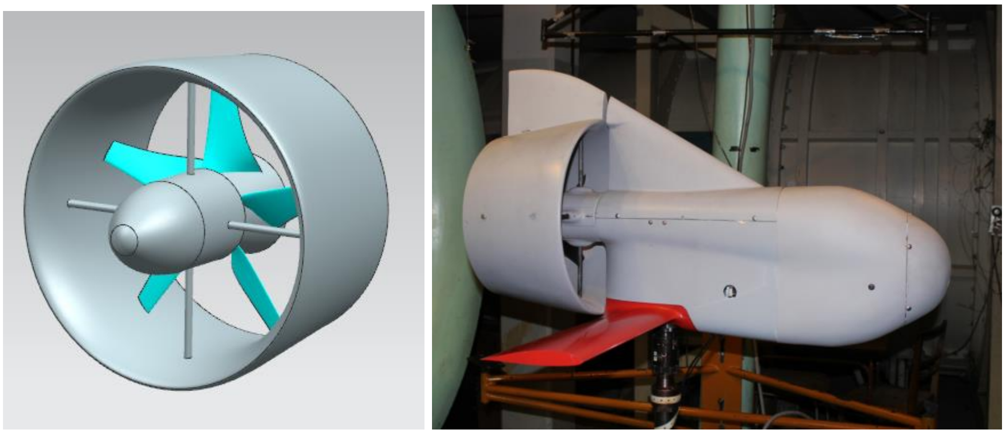

Fig.2. First version (V1) of the propulsion system

After gaining knowledge and experience, new version (V2) of the ducted fan unit has been designed (Fig.3). Main visible difference is the chord length of the duct (0,12m compared to 0,25m of its predecessor). As the same fan has been used, the internal diameter stayed the same -0,35m.
This leads to lower weight, but more difficulties in the design of the structure of the duct.
As significant influence of the rods holding the duct on the fan’s performance in V1 is present, V2 has them further separated from the fan.

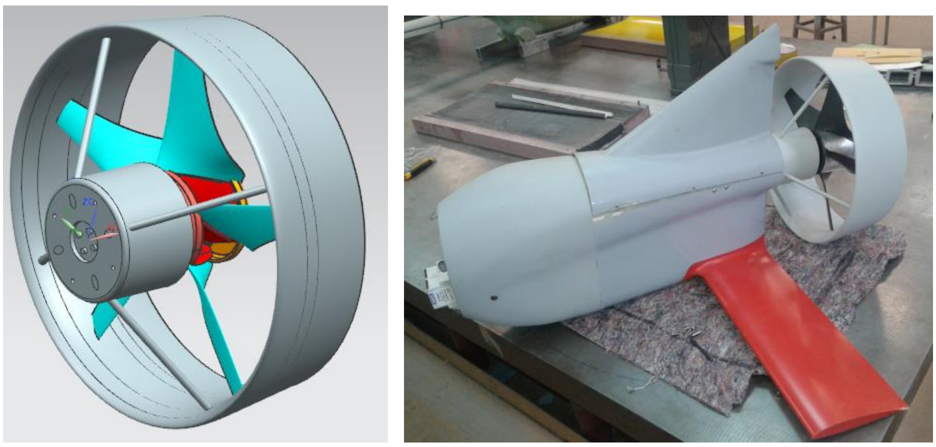

Fig.3. Second version (V2) of the propulsion system

2. WIND TUNNEL TESTS

2.1 Wind tunnel

Wind tunnel tests have been performed in the T-1 aerodynamic tunnel which belongs to the Institute of Aviation in Warsaw, Poland. The wind tunnel has a diameter of 1.5m and allows speeds ranging from 12 up to 45m/s. The tunnel is using a 55kW electric motor powering a 4 blade constant speed fan. The speed is controlled by changing the angle of the blades (for higher changes) and special flaps (for precise control of the speed).

Fig.4. T-1 wind tunnel

2.2 Wind tunnel test object

As the conditions in which the ducted fan is working are not typical (pusher propeller with the fuselage in front), a model simulating them has been prepared. It consisted of last 0,4m of the rear of the fuselage together with the vertical fin and added nose section (Fig. 5). What is more, aft wing has been included with about one third of the wingspan.

Fig.5. The investigated object in the T-1 wind tunnel, with V1 ducted fan

The investigated fan was powered by the 3kW brushless electric Turnigy motor. The rotational speed of the fan was controlled by a 120A Electronic Speed Control unit and the National Instruments USB-6211 I/O card. Battery setup consists of 24 LiFe cells in 12s2p configuration (12 cells parallel, 2 in series) giving 44,4V fully charged. All the electronic equipment was mounted inside the fuselage.

The aerodynamic loads, acting on the complete model, have been measured by the HWG-6 strain-gage balance, which is a part of the mount of the model. The balance is placed vertically (perpendicular to the duct's axis) and such placement does not allow the excess of its limits during tests. The performance of the power unit (i.e. thrust, torque, rotational speed and electric current and voltage) has been measured by a specially designed test stand. The stand has been used only when the engine was turned on.

As several different configurations have been considered, repeatability of the tests was necessary to get comparable data. A special program for running the motor has been written using the Lab View software.

3. COMPUTATIONAL FLUID DYNAMICS ANALYSES

As it is very hard or even impossible to gain some type of data from wind tunnel like drag on each particular part for example rods or the duct, it has been decided that a 3D model for computational fluid dynamics (CFD) has needed to be done (fig.6). The basic model consists of two domains: The outer which is the air closed by the walls of the cylinder and the inner consisting of the air in which the fan rotates (crosshatched in fig.6). They are joined with interfaces in which the air from both of the domains mixes. Flat inlet gives good results for only very small angles of attack, but gives much better and more precise mesh. To simplify the model, the fuselage and wing in front of the propulsion system has not been modeled and instead has been replaced by a nose cone. Until now only the V1 version of the fan has been modeled.

The CFD model consists of 1,7 million cells (together with boundary layer) and the turbulence model has been set to Spalart-Allmaras. In order to verify the assumptions and settings of the analysis the model has been tested in free stream speed of 25m/s and maximum rotational speed of 6800 rpm, which matched the settings used in the wind tunnel (max. power at cruise speed). The results of the thrust (negative value of drag) did not differ more than 10%. The difference between the values mainly comes from the unmodeled fuselage in the front which changes the inlet airflow, so the model has been treated as verified.

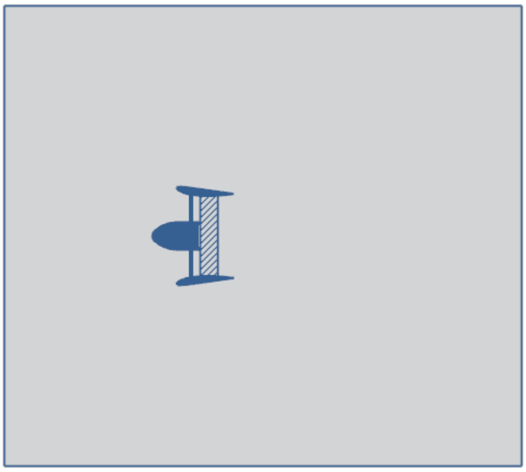

Fig.6. The cross section of the model.

As the rotational speed during free spin tests in the wind tunnel has not been measured, it had to be derived from CFD analyses. As it is possible to calculate the forces and moments on each separate element of the model, several simulations for different rotational speeds of the fan have been evaluated. In the place where the torque of the fan is equal to zero, the fan is neither "powered" by the free stream, nor "powered" by the motor and if efficiency and friction in the bearings are not taken into account the result should be accurate enough. In this case the value of torque equal to zero corresponds to rotational speed of n~3800 [1/min]. Further calculations for this rotational speed are being presented further in this paper. The free stream velocity was V_t=25 [m/s]

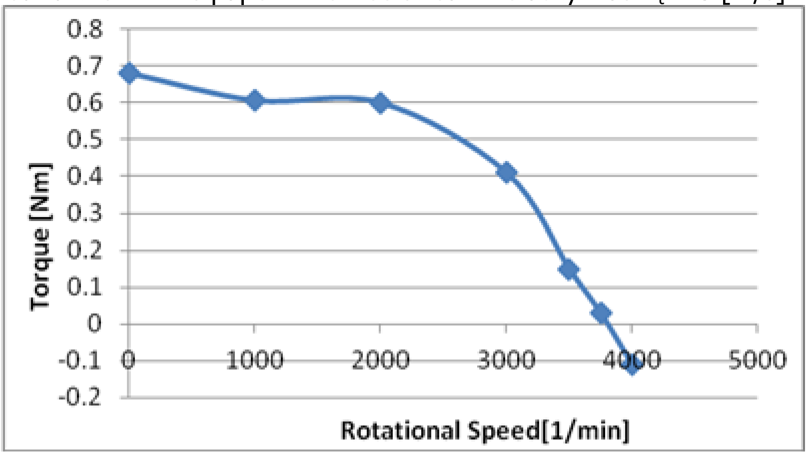

Fig.7. Torque in function of rotational speed used to determine to rotational speed of free spinning fan

4. RESULTS

4.1 Wind tunnel

During the wind tunnel tests, the drag of the ducted fan (in V2 version) has been obtained for free-wheeling and locked fan for various speeds of the wind tunnel's stream flow. The drag force of the fuselage and duct (with disassembled fan) has been obtained as well. It has been plotted (as a function of the dynamic pressure of the freestream)) in Fig. 8. The dynamic pressure is given by the typical formula:

$$q = \frac{\rho \cdot V^2}{2}\text{, where}$$

P=density of air
V-velocity of the free stream

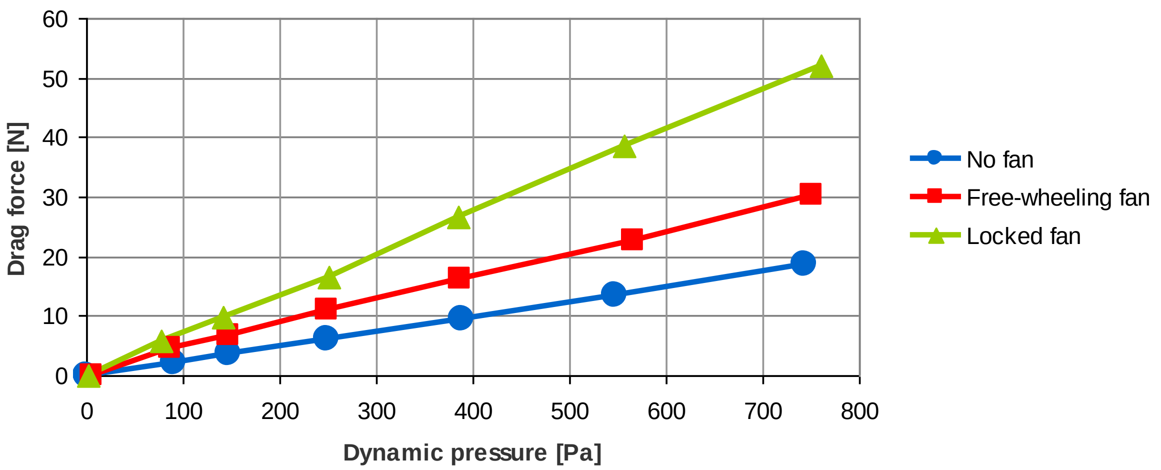

Fig. 8. Drag force vs freestream dynamic pressure

According to the plot in Fig. 8, the drag coefficient in every case was nearly constant (a drag force is a linear function of the dynamic pressure of the freestream). The drag coefficient, referred to the fan disc area, has been presented in the Table. 1:

	No fan	Free-wheeling fan	Locked fan
C_D	0.0697	0.1153	0.1932
ΔC_D	-	0.0456	0.1235
$\Delta C_D / C_{D\ fuselage}$ [%]	-	65.32	177.02

Table 1. Drag coefficient of the fuselage and V2 fan (free-wheeling and locked)

Both free-wheeling and locked fan gives a significant drag: 65% and 177% of the fuselage drag, respectively.
The results in Table 1 consider only the V2 version, i.e. the duct with reduced chord (from 0.25 m to 0.12 m). Drag coefficient values for V1 and V2 versions, without the fuselage drag have been presented in Table 2.

		V1 fan	V2 fan	Difference [% of V1]
C_D	Fuselage + duct	0.2615	0.2449	6.33
	Free-wheeling fan	0.4917	0.4279	12.97
	Locked fan	0.7901	0.7027	11.06
ΔC_D	Free-wheeling fan	0.2302	0.1830	20.52
	Locked fan	0.5287	0.4578	13.41

Table 2. A comparison of the drag coefficient of both versions of the propulsion unit

According to the Table 2, the drag coefficient of the free-wheeling fan is 20% lower in the V2 version, and the drag of the locked fan is 13% lower. These values are significantly better than the difference of the drag coefficient of the fuselage and duct (which has been reduced of over 6%).
Both versions of the ducted fan have been compared with a reference propeller used typically in radio controlled model airplanes- Fiala 20”x10”. This propeller has been chosen because of the static thrust and power level similar to the designed ducted fan. It must be noted that the propeller had significantly higher diameter (20 inches instead of 14 inches). In this case, drag coefficients related to the disc area would not be reliable – it is better to compare only the values of the drag force. The comparison has been presented in Table 3 and Fig. 9.
For each of the following measurements, the free stream velocity was V_t=25[m/s].

		V1 fan	V2 fan	Propeller
Drag [N]	Fuselage	7.5	7.5	7.5
	Duct	2.5	1.8	-
	Free-wheeling fan	18.7	16.3	13.9
	Locked fan	30.1	26.8	12.1
ΔDrag [N]	Free-wheeling fan	8.8	7.0	6.3
	Locked fan	20.1	17.4	4.6

Table 3. A comparison of the drag of the ducted fan and the propeller

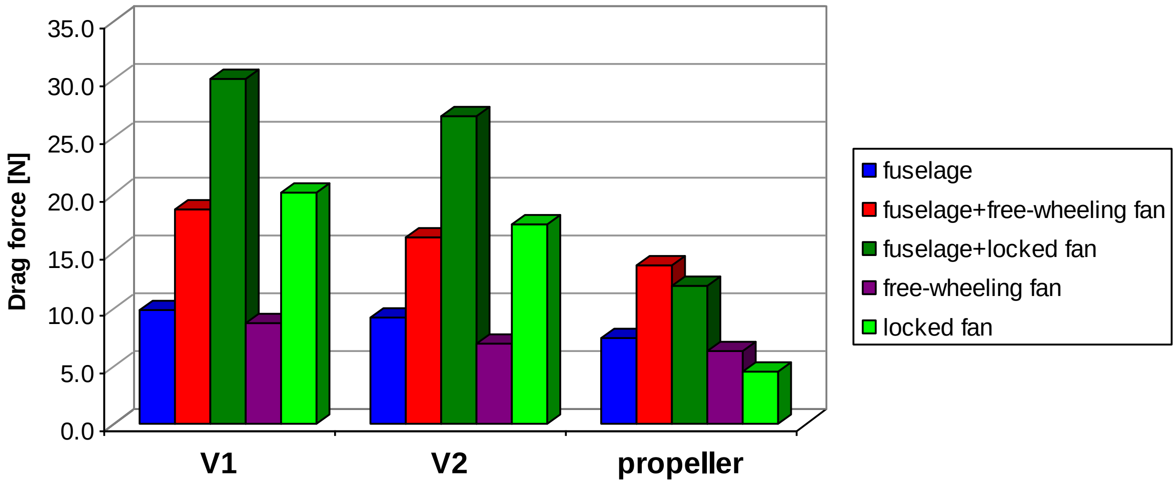

Fig. 9. A comparison of the drag of the ducted fan and the propeller

The drag of the free-wheeling fan (for the V2 version) is similar to the drag of the free-wheeling propeller. However, the drag of the propeller may be reduced by locking it, while locking the ducted fan would give an opposite effect – a significant increase of the drag. It may be caused by a large blockage of the flow inside the duct by the locked fan.

4.2 Computational Fluid Dynamics

As an addition for the wind tunnel investigation, CFD analyses of a simplified model (without the part of the fuselage in fron of the ducted fan) have been performed. The analysis was aimed on obtaining the drag force acting on each part of the simplified model, i.e. fan, duct, nose cone and rods. Value of the drag for the whole system for the free-wheeling scenario obtained in the CFD analysis is 11,08N, which is just slightly smaller than the value obtained in wind tunnel tests (11.2N).

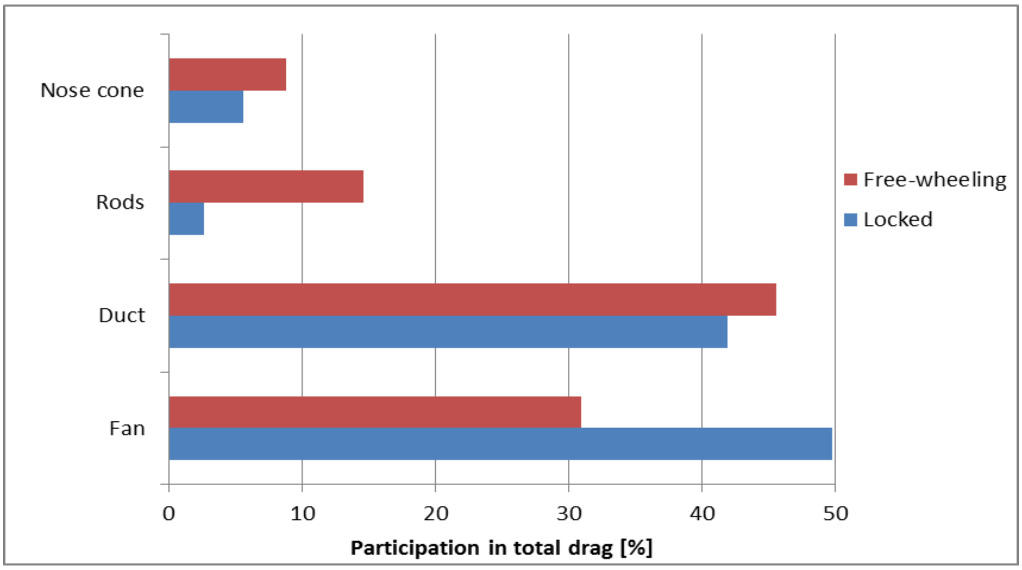

Fig.10 Participation of each individual part in total drag force of the propulsion system

In order to show how each individual part of the propulsion system affects the total drag, bar graph has been prepared (fig.10). The graph shows that the drag force of the duct and the nose cone has the least influence on the total drag. The drag force of the fan is greatly reduced when it rotates, which is what the research has been mostly focused on. What might be very surprising is the high growth of the drag force of the rods on the whole system when the fan rotates, it might be caused by the influence of the fan itself. The second version of the fan has the rods spread further from the fan and it still needs to be analyzed if this section has been improved.
Fig.11 shows one of the visualization plots of the streamlines during the free-wheeling phase.

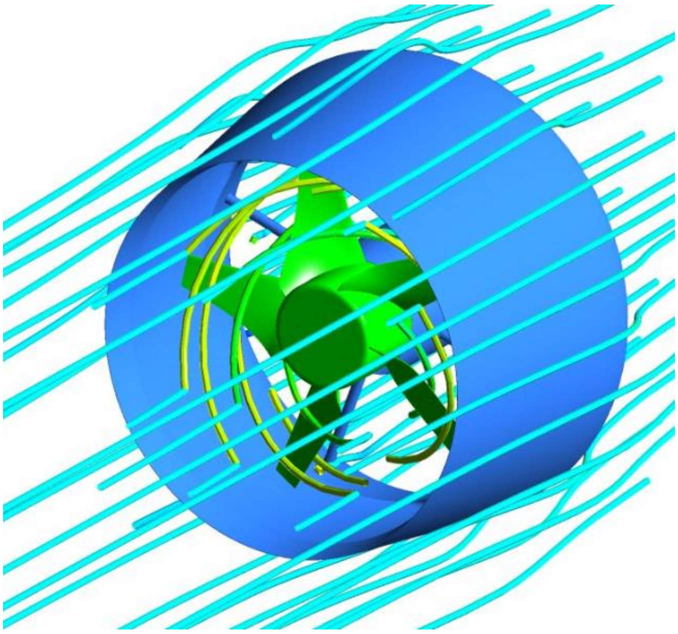

Fig.11. Visualization of the airflow at n=3750 [1/min]

5. SUMMARY

The drag force acting on the non-powered ducted fan is significant and must be taken into account in the phase of propulsion design. In opposite to propellers, a locked fan may cause a significantly higher drag than the free-wheeling one. It is connected with a reduction of aircraft performance. For example, the glide ratio of MOSUPS aircraft decreases from 10.5 to 9.5 (reduction of 10%) and minimum sink velocity increases from 1.39 m/s to 1.54 m/s (increment of 11%). The polar curves of MOSUPS aircraft are being presented in Fig. 12.
It must be noted that this effect has been observed both on an isolated ducted fan (i.e. without a fuselage) investigated numerically and on the ducted fan with a fuselage, tested in the wind tunnel.
In order to fully understand the reason of the differences in the drag caused by stationary and free-wheeling fan further CFD analysis has to be conducted. It is also planned to do a smoke visualization and PIV tests in the wind tunnel.

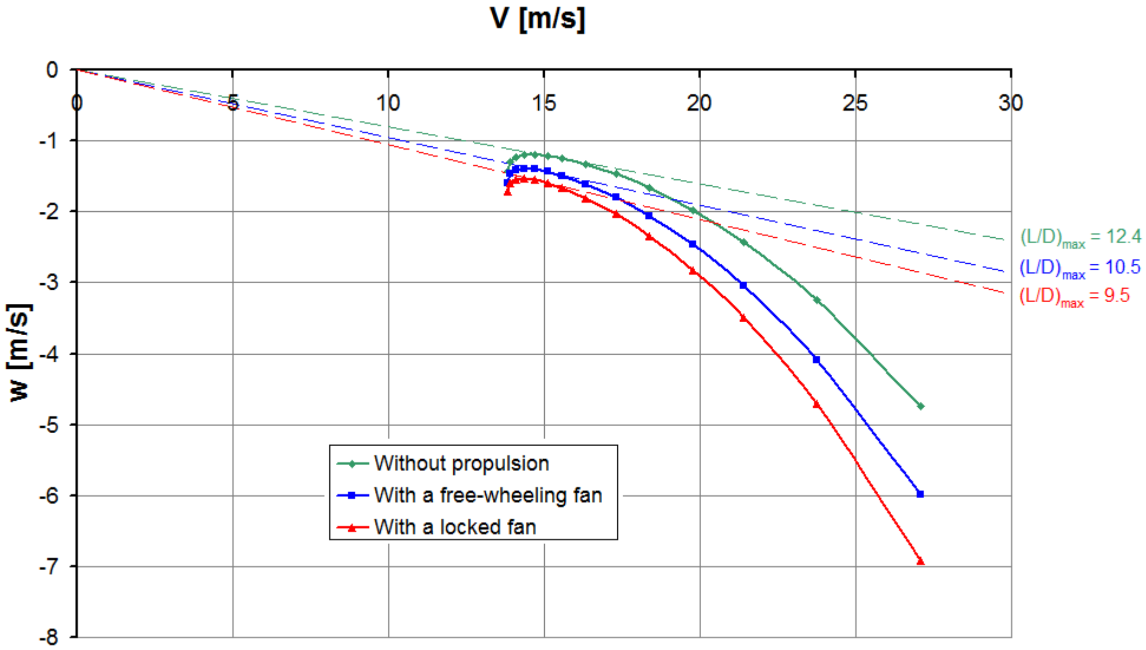

Fig.12. Polar curves of the MOSUPS aircraft

ACKNOWLEDGEMENTS

The authors would like to acknowledge all colleagues from the MOSUPS project partners who contributed to the success of the collaborative design studies that provided valuable input for the research described in this paper.

This work was supported by The National Centre for Research and Development under grant No. PBS/A6/14/2012.

REFERENCES

[1] Bogdański K., Krusz W., Rodzewicz M., Rutkowski M. – Design and Optimization of Low Speed Ducted Fan for a New Generation of Joined Wing Aircraft. 663 paper in proceedings of the ICAS'2014 conference, St. Petersburg, 7-12 September 2014

[2] Bogdański K., Rodzewicz M., Ruchała P., Miller M. – Concept and realisation of propulsion system tests in a wind tunnel. Mechanika w Lotnictwie ML-XVI, 2014 (in Polish)

[3] Bogdański K., Rodzewicz M. - Integration of the propulsion system with MOSUPS aircraft. READ 2014 conference, Vilnius

[4] Galiński C., Krysztofiak G., Lis M., Kalinowski M., Stefanek L., Hajduk J. – Selected issues of the joined wing scaled demonstrator investigation programme. Mechanika w Lotnictwie ML-XVI, 2014 (in Polish)